Stress Testing for Performance Analysis of Orientation Estimation Algorithms

Giovanni Betta, *Senior Member, IEEE*, Domenico Capriglione, *Senior Member, IEEE*, Marco Carratù, *Member, IEEE*, Marcantonio Catelani, *Member, IEEE*, Lorenzo Ciani, *Senior Member, IEEE*, Gabriele Patrizi, *Member, IEEE*, Antonio Pietrosanto, *Senior Member, IEEE*, and Paolo Sommella, *Member, IEEE*

***Abstract*— Technological advancements have seen the spread of micro-electromechanical systems (MEMSs) based sensors such as inertial measurement unit (IMU) systems. The latter provide object orientation information in numerous applications such as smartphones, robotics, automotive, drones, and many others. In more detail, IMUs based on MEMS technology are characterized by small size, low power, and low cost. Technically, orientation information is provided by appropriate orientation estimation algorithms fed with quantities measured by MEMS sensors, such as acceleration, angular velocity, and magnetic field. A preliminary work pointed out that such MEMS sensors suffer significant drifts when they have to endure non-standard operating profiles in terms of thermal conditions. However, when considering very low-cost devices, the influence of temperature on the operation of orientation estimation algorithms still remains an important research gap in the literature. To deal with this important aspect, this article proposes a specific test plan to analyze the performances of MEMS-based IMUs by considering a temperature stress test. Therefore, the effect of temperature was first analyzed on the individual sensors of the IMU (accelerometer, gyroscope, and magnetometer), then the effects of a very simple temperature compensation strategy were analyzed to highlight the importance of such step. Specifically, the effects of not compensating for temperature were studied considering a low-cost commercial IMU typically used in various fields of application. To better quantify such effects in practical applications, two well-known orientation estimation algorithms (i.e., complementary filter and attitude and heading reference system (AHRS) typically fed by IMUs output have been considered. The experimental results obtained using the custom devices under test (DUTs) show that temperature compensation is necessary for the best performance of the analyzed orientation estimation algorithms.**

***Index Terms*— Fault diagnosis, inertial navigation, reliability, temperature dependence, testing.**

I. Introduction

INERTIAL measurement units (IMUs) are essential platforms in modern technologies used to measure several physical quantities, such as angular velocity, linear acceleration, and static magnetic field [1].

Smartphones and tablets (and, more generally, all consumer electronics) are one of the biggest markets for implementing low-cost and low-power IMUs. Examples of applications are human activities recognition [2], real-time smartphone activity classification [3], and positioning identification [4]. In addition, several other industrial and technological fields strongly rely on using IMUs. Few examples are verticality measurement [5], wearable sensors for human locomotion patterns recognition [6], automotive applications (such as self-driving vehicles [7] and motorcycles [8]), aeronautical technologies (such as UAVs–unmanned aerial vehicles [9] and submarines drones [10]), robotic equipment (e.g., biomedical units or manufacturing devices, as in [11] and [12]), wearable technologies to assess standing balance [13], and data acquisition during sports activities [14].

The leading manufacturing technology in the IMUs market has been rapidly driven toward micro-electromechanical systems (MEMSs) units. As a result, the accuracy and stability performances of low-cost, low-power, low-dimension MEMS-based IMUs rapidly increase, leading to a reliable solution for acquiring data [15]. For instance, Wang et al. [16] proposed an autonomous MEMS-based IMU to evaluate rotary in-drilling alignment able to operate under severe environmental conditions, while in [17], a MEMS-based IMU was used for train positioning.

Depending on the field of application, numerous external stresses (e.g., thermal excursion, humidity exposure, wideband random vibration, mechanical over-shocks, and many others) influence the IMU's performance and significantly affect the reliability of their output. Thus, it is becoming fundamental to study the metrological performance of sensors and instrumentations in the presence of such external stimuli.

According to several works in recent literature, temperature excursions and, more generally, any thermal stresses represent the main influence factor on the functional and metrological performances of any electronic devices, such as power modules [18], accelerometers [19], technologies applied in the Internet of Things (IoT) [20], capacitive flow meters [21], and many others.

With more reference to MEMS-based IMU, the authors show a remarkable dependency between the IMU's output and the operating temperature in preliminary works published in [22] and [23]. They present the experimental results of 9 degrees of freedom (DoF) MEMS-based

Manuscript received 30 July 2022; revised 30 September 2022; accepted 8 October 2022. Date of publication 21 October 2022; date of current version 7 November 2022. The Associate Editor coordinating the review process was Dong Wang. *(Corresponding author: Lorenzo Ciani.)*

Giovanni Betta and Domenico Capriglione are with the Department of Information and Electrical Engineering "Maurizio Scarano", University of Cassino and Southern Lazio, 03043 Cassino, Italy (e-mail: betta@unicas.it; capriglione@unicas.it).

Marco Carratù, Antonio Pietrosanto, and Paolo Sommella are with the Department of Industrial Engineering, University of Salerno, 84084 Fisciano, Italy (e-mail: mcarratu@unisa.it; apietrosanto@unisa.it; psommella@unisa.it).

Marcantonio Catelani, Lorenzo Ciani, and Gabriele Patrizi are with the Department of Information Engineering, University of Florence, 50139 Florence, Italy (e-mail: marcantonio.catelani@unifi.it; lorenzo.ciani@unifi.it; gabriele.patrizi@unifi.it).

Digital Object Identifier 10.1109/TIM.2022.3216400

IMU units (i.e., 3-axis accelerometer, 3-axis gyroscope, and 3-axis magnetometer) characterized under temperature variation within the operating ratings compliant with the datasheet of the device under test (DUT). Furthermore, the papers emphasize how this strong correlation has been measured on the output of the accelerometer, gyroscope, and magnetometer for every considered axis orientation and every IMU under test.

The temperature stress presented in the previous works triggered no failure mechanisms, and no significant effects on system reliability have been discovered. The most striking results in the preliminary works are the presence of miss-calibrations and loss of compensations, even if the temperature stress is entirely inside the device's operating temperature range. Furthermore, the propagation of even minor temperature miss-compensations in terms of raw data acquired by the sensors seems to remarkably affect the results provided by common filtering algorithms employed in positioning applications [22], [23]. Despite that, the IMU manufacturer only states the presence of a possible linear dependency with temperature, missing the consideration of important characterization in the device documentation. As a matter of fact, no calibration procedures for temperature excursions are suggested, as well as no mathematical formulations of temperature-output correlation are available to correct these unwanted effects.

Therefore, the accurate evaluation of the systematic and aleatory errors induced by the actual operating conditions (i.e., temperature stress) on the performances of orientation estimation algorithms represents a key research gap that must be investigated. Such analysis should lead to the development of ad hoc self-calibration procedures for every considered IMU. Few works in recent literature tried to propose temperature correlation analysis and temperature compensation on MEMS-based sensors; however, to the authors' knowledge, a complete characterization covering a 9-DoF MEMS-based IMUs (i.e., accelerometers, gyroscopes, and magnetometers) under cold and hot temperatures is also currently missing as a thorough analysis of the effects that such stresses have on the performance of typical orientation estimation algorithms.

For instance, the correlation between temperature and the output of MEMS-based IMUs has been studied by Altinoz and Unsal [24]. In such a paper, a temperature step-test emphasizes that five temperature points are sufficient to compensate for the deterministic error caused by temperature drifts adequately. An innovative stability error modeling for MEMS-based IMU based on the correlation of low pass filtered sensor outputs has been developed and validated in [25], focusing only on positive temperatures. Hoflinger et al. [26] developed a 9-DoF wireless micro IMU using MEMS technology and featuring automatic temperature compensation in a single chip, while Yang et al. [27] developed a micro oven-control system to compensate thermal drifts in 6-DoF commercial IMUs. Araghi and Landry [28] introduce an innovative approach for temperature compensation (deterministic error of both accelerometer and gyroscope) based on a radial basis function neural network (RBFNN).

Some papers in recent literature focus only on the temperature compensation of MEMS gyroscopes without dealing with the other sensors commonly integrated inside an IMU. For instance, Tu and Peng [29] propose an ARMA-based Digital Twin solution, while Fontanella et al. [30] use a backpropagation neural network algorithm. Zhang et al. [31] present a comparison between the traditional calibration method and the proposed parameter-interpolation calibration method, while in [32], the problem of gyroscope temperature compensation has been solved by investigating the gyroscope scale factors errors. Quite the opposite, Gunhan and Unsal [33] suggest several polynomials with different degrees to compensate for temperature effects, focusing only on the accelerometer's output.

In this framework, considering the preliminary experimental results given in [22] and [23], this article presents a customized temperature test plan and a suitable experimental setup to investigate the temperature miss-compensation of low-cost MEMS-based IMU units. In addition, the proposed test also aims to analyze the effects of a temperature dependency compensation on well-known orientation estimation algorithms.

The major contributions of this research are the following.

1) Investigating temperature drifts and miss-compensation phenomena on low-cost MEMS-based IMUs in a controlled operating environment specifically customized for these kinds of devices.
2) Discussion of the effects of IMU's output anomalies due to temperature and the correlation of such behaviors with the orientation of the IMU itself (and thus with the axis of application of the gravitational acceleration), which has never been previously discussed in the literature. To do that, the proposed test has been repeated three times, one for each possible orientation (i.e., X-axis, Y-axis, and Z-axis).
3) Systematic and thorough discussion of the temperature error analysis and compensation on all the sensors and all the axis of a 9-DoF MEMS-based IMU.
4) Evaluation of temperature compensation effects on two common orientation estimation algorithms, such as complementary and attitude and heading reference system (AHRS) filters. This analysis allowed to cover a research gap regarding the accuracy of the orientation estimation when the sensors operate under nonstandard operating conditions.

II. Proposed Temperature Test Plan

Several different application fields of MEMS-based IMUs are characterized by cold-hot thermal variations in a wide temperature range. For example, this is the case with automotive technologies, UAVs, and submarine drones, to cite a few. Low-cost consumer electronics could also, however, be subjected to temperature drifts and hot and cold exposure. Currently, no specific standards are available for environmental testing and metrological characterization of either MEMS sensors or IMU units. Thus, the proposed test plan is based on a variety of general and field-specific standards regarding environmental testing procedures but is tailored to the explicit purpose of thermal calibration and correction of miss-compensations of low-cost commercial MEMS-based IMUs. Some of the main reference standards consulted during the draft of the proposed test plan are the following.

TABLE I
TEMPERATURE SET POINT OF THE PROPOSED TEST PLAN

TYPE OF STRESS	NOTATION	TEMPERATURE SET POINT
Hot Temperature exposure	T_H	50 °C
Cold Temperature exposure	T_C	-10 °C
Ambient Temperature (reference condition)	T_A	20 °C

1) The entire IEC 60068-2 series [34]. This collection of international standards describes how to implement different kinds of environmental testing, including hot and cold temperature stresses.
2) The test guideline MIL-STD-810G [35] is a milestone and reference guideline for all types of environmental test laboratories.
3) The JESD22 A104E [36] standard for temperature cycling test of microelectronics devices.
4) The AEC-Q100 [37] standard for stress test qualification (including temperature stress profiles) of electronic devices used in automotive applications.
5) The European standard ETSI EN 300 019-2-5 [38] covers the testing procedure for installing electronic and telecommunication units on terrestrial vehicles).
6) The ISO 16750-4 [39] international standard deals with environmental testing procedures of electronic and electric devices mounted on-road vehicles.

Aiming at error corrections due to temperature drifts, the proposed procedure uses a climatic chamber to regulate the temperature of the DUTs considering three setting temperatures, as in Table I. A preliminary preconditioning phase at reference conditions T_A is required to perform some pretest measurement in a standard environment. After that, the proposed temperature cycle starts as follows.

1) First, the temperature inside the climatic chamber is lowered until reaching the cold exposition temperature T_C. The decreasing temperature rate is set equal to -2 °C/min to gradually cool the devices.
2) When the cold temperature T_C has been reached inside the chamber, the automatic measurement setup shall stabilize the exposition temperature and keep it constant at -10 °C for an exposition time of 30 min.
3) The following phase is a slow and gradual increase of temperature from the cold exposition temperature T_C up to the hot exposition temperature T_H. Similar to the previous case, the temperature increase rate is set equal to 2 °C/min.
4) After reaching the hot temperature T_H inside the chamber, an exposition phase at a constant hot temperature of 50 °C is maintained for an exposition time of 30 min.
5) After that, the final step of the cycle is a cooling phase performed at a slow decrease rate (i.e., -2 °C/min) until ambient temperature is reached.
6) Finally, the cycle ends with another exposition phase at ambient temperature T_A performed for 30 min. In this phase, the operation of the DUT shall return to standard conditions.

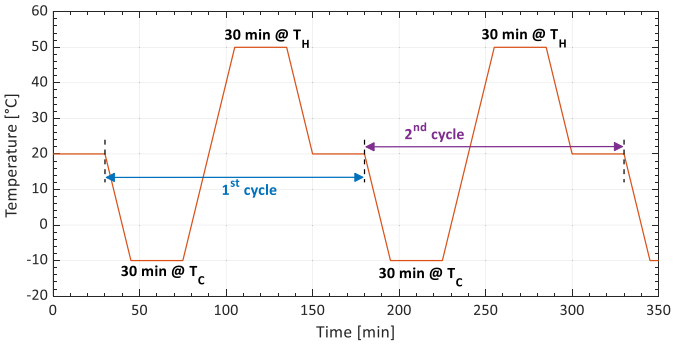

Fig. 1. Proposed temperature test plan for calibration and temperature compensation of IMU systems. For the sake of illustration, only the first part of the test has been illustrated (i.e., a preconditioning phase and two consecutive cycles). The entire test profile includes two other temperature cycles and the final measurement and inspection phase.

The six test steps described above stand for a complete temperature cycle. For the sake of repeatability, four consecutive repetitions of the proposed temperature cycle have been performed. The test profile instead refers to the whole test, including the preconditioning phase, four temperature cycles, and a final inspection and measurement phase of 30 min. The estimated duration of the complete test profile is approximately 12 h.

A portion of the entire test plan is illustrated in Fig. 1, showing only the first two consecutive cycles.

One of the significant innovations of the proposed test plan is that the complete temperature test profile must be repeated three times. This redundancy is not due to repeatability issues as the repetition of four consecutive cycles described above. Instead, the three repetitions of the test profile are required to investigate the effect of the gravitational acceleration on the three axes of the considered IMU. To do that, each repetition changes the device's orientation toward a different axis (X, Y, and Z, respectively). In this way, it is possible to study and analyze the effects of miscalibration and temperature drifts and their correlation with the constant gravitational acceleration (and thus with the device's orientation).

The proposed temperature-based test plan has been developed taking into account the aim of the work, which is the characterization of low-cost IMUs (in terms of both raw data and orientation estimation algorithms) for commercial applications (such as low-cost drones, smartphones, and the automotive field). Thus, the test severity (in terms of temperature set point, temperature profile, temperature rate, etc.) has been customized on this application. For instance, higher temperature rates during heating and cooling phases are not suitable in this work to ensure that the temperature profile is a good representative of the actual operating conditions in the considered applications.

III. EXPERIMENTAL SETUP

The DUTs are a set of low-cost commercial 9-DoF MEMS-based IMU able to acquire data about linear acceleration, angular rate, and magnetic field toward three axes. The key features of the system-in-package IMUs under test are summarized in Table II.

TABLE II
KEY FEATURES OF THE LOW-COST MEMS-BASED IMUS TESTED

FEATURE	VALUE
Accelerometer channels	3
Gyroscope channels	3
Magnetometer channels	3
Linear acceleration full scale	±2 g ±4 g ±8 g ±16 g
Angular rate full scale	±245 DPS ±500 DPS ±2000 DPS
Magnetic field sensor full scale	±4 gauss ±8 gauss ±12 gauss ±16 gauss
Output data	16 bit
Interfaces	SPI I2C
Supply voltage	1.9 V to 3.6 V
Other embedded sensors	Temperature transducer
Operating temperature range	-40 °C to +85 °C

The IMUs under test have been integrated into a self-designed board used to host and supply the IMU and to interface the sensors with the external acquisition chain. The latter comprises an STMicroelectronics Nucleo-64 board (used to initialize the sensors and manage the I2C-based communication) and a laptop (used to collect and store the data). Both Nucleo-64 and the laptop are used only for data acquisition and storage and are not the object of the calibration analysis.

Thus, they should not be exposed to the temperature stress test. In this way, it is possible to guarantee that any temperature drift and miss-calibration phenomena derived only from the IMUs under test are entirely unrelated to the acquisition unit maintained at a constant temperature during the whole test duration. A set of three MEMS-based IMU, described in Table II, have been located inside a climatic chamber able to regulate the temperature in compliance with the specification of the proposed test plan described in Section II. The measurement setup also includes a data logger equipped with two PT100 resistance temperature detectors (RTDs) and three T-type thermocouples. The RTD sensors are used to monitor the temperature variation inside the climatic chamber. At the same time, the thermocouples are placed in direct contact with the IMU to evaluate the system overheating. A schematic representation of the proposed measurement setup is illustrated in Fig. 2, while a picture of the actual deployment inside the chamber is shown in Fig. 3. The latter also highlights the different orientations toward the three axes in which the DUTs have been tested. Note that the picture is for illustration only, while the actual test has been repeated three times, using three devices in each of the three possible orientations in Fig. 3.

It is also important to note that the following key aspects are essential to guarantee the repeatability of the experiments: the accuracy of the temperature regulation within the chamber used for testing (in this work, the accuracy of the temperature control is ±0.3 K); the correct installation of

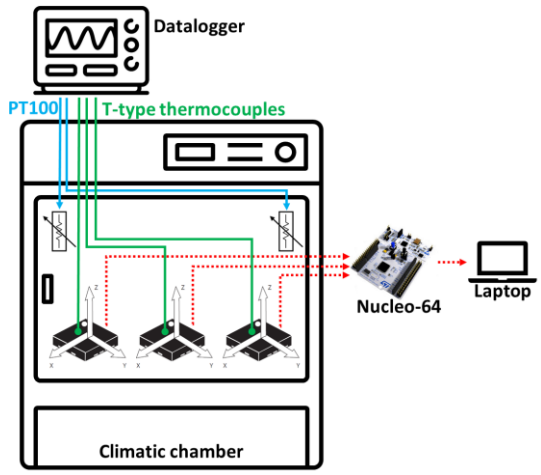

Fig. 2. Schematic representation of the proposed experimental setup, including a climatic chamber, a datalogger, RTDs, and T-type thermocouples, along with the IMUs under test and the acquisition chain.

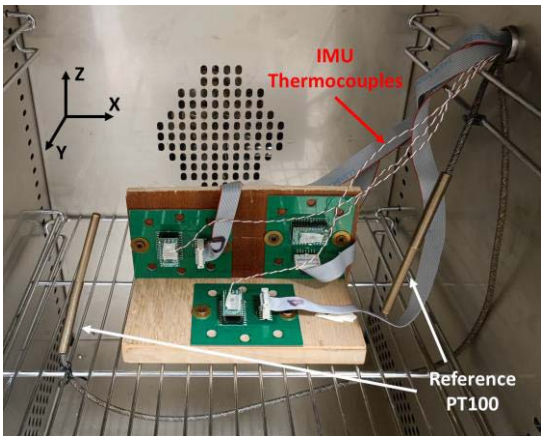

Fig. 3. Picture of the actual measurement setup highlighting the three different orientations of the devices toward the X, Y, and Z axis.

the thermocouples; and the correct positioning of the devices toward perpendicular axes to cover the three different directions monitored by the IMUs.

IV. TEMPERATURE INFLUENCE ANALYSIS

The first analysis regarding the temperature influence has been done by evaluating the variation of the IMU sensors' output during two successive observation windows, including a quiet zone at an ambient temperature equal to $T_A = 20$ °C and the test zone described in Section II. Tables III–V show the behavior exhibited by a single triaxial sensor output (each table refers to a different DUT) during four repetitions (i.e., $R1$, $R2$, $R3$, and $R4$ for each orientation of the DUT) of the proposed thermal cycle. The empirical distribution's main statistical parameters (i.e., minimum, maximum, mean, and standard deviation) corresponding to each observed signal during the controlled temperature cycle are reported. The acquired data have also been compared to the values achieved when the DUT works at ambient temperature (the latter condition has been considered as a reference). As a matter of fact, the temperature

TABLE III
ORIENTATION TOWARD THE X-AXIS. MINIMUM, MAXIMUM, MEAN, AND STANDARD DEVIATION OF (DUT1) SENSOR OUTPUTS VERSUS TEMPERATURE CYCLES

GYROSCOPE [dps]																				
	Reference				R1				R2				R3				R4			
AXIS	Min	Max	Mean	σ	Min	Max	Mean	σ	Min	Max	Mean	σ	Min	Max	Mean	σ	Min	Max	Mean	σ
x	-0.02	-0.01	-0.02	0.00	-0.02	0.11	0.05	0.04	0.01	0.05	0.03	0.00	-0.06	0.01	-0.03	0.02	-0.46	0.02	-0.02	0.01
y	-0.09	-0.05	-0.08	0.01	-0.12	0.15	0.00	0.06	-0.07	0.20	0.07	0.04	-0.10	0.14	0.03	0.03	-0.08	0.19	0.04	0.04
z	-0.02	-0.01	-0.01	0.00	-0.04	-0.01	-0.03	0.01	0.01	0.05	0.03	0.01	0.01	0.05	0.03	0.01	0.05	0.09	0.06	0.03

ACCELEROMETER [m/s^2]																				
	Reference				R1				R2				R3				R4			
AXIS	Min	Max	Mean	σ	Min	Max	Mean	σ	Min	Max	Mean	σ	Min	Max	Mean	σ	Min	Max	Mean	σ
x	5.19	10.03	9.56	0.52	5.09	10.36	9.71	0.24	5.18	10.76	9.82	0.17	5.23	10.95	9.65	0.27	5.03	10.90	9.55	0.37
y	0.06	0.17	0.15	0.01	-0.42	0.45	0.04	0.14	-0.75	0.59	-0.05	0.16	-0.49	0.41	-0.09	0.12	-0.40	0.36	-0.06	0.21
z	-0.38	-0.19	-0.36	0.02	-1.55	0.47	-0.35	0.28	-1.12	0.37	-0.37	0.14	-1.47	0.70	-0.42	0.28	-1.68	0.69	-0.24	0.27

MAGNETOMETER [nT]																				
	Reference				R1				R2				R3				R4			
AXIS	Min	Max	Mean	σ	Min	Max	Mean	σ	Min	Max	Mean	σ	Min	Max	Mean	σ	Min	Max	Mean	σ
x	-34.63	-17.68	-32.80	1.79	-53.16	-17.97	-43.67	6.43	-108.12	-3.75	-79.51	8.27	-71.24	-25.53	-60.63	6.94	-62.42	-23.59	-58.98	5.34
y	-17.99	-9.18	-17.00	0.93	-15.65	0.75	-7.19	4.97	0.19	29.19	12.91	6.89	-35.35	-15.63	-24.22	4.84	-37.53	-18.35	-27.44	4.28
z	-3.23	-1.12	-2.68	0.34	-23.44	-2.10	-13.00	6.83	71.35	203.36	141.76	21.46	-118.95	-51.16	-108.10	6.84	-108.36	-42.65	-119.01	7.01

variation of the proposed test influences all sensors' outputs, particularly the magnetometer and the gyroscope. This behavior is mainly highlighted by the considerable difference in the excursion range measured (minimum and maximum values) and the variation observed for the standard deviation of sensor outputs among the different analysis zones.

Indeed, in summary from Tables III–V, an absolute maximum range of sensors output can be observed due to the temperature test proposed of 0.31 dps for the gyroscope, 5.92 m/s^2 for the accelerometer, and 132.01 nT for the magnetometer, respectively.

Further interesting results can also be drawn and are reported in the following: 1) whatever be the sensor, the temperature influence is not correlated with the three different orientations and 2) the temperature influence is similar, whatever be the considered IMUs (respectively, the x, y, and z axis toward the gravity vector, as illustrated in Fig. 4 for a single temperature cycle).

Each analyzed IMU, however, shows a different relationship with the temperature changes, as can be retrieved by evaluating the noncompatibility from a measurement point of view. Thus, a temperature compensation procedure is really advisable before using the data in further applications, such as the algorithms for orientation estimation.

V. TEMPERATURE COMPENSATION

To compensate for the temperature effects on sensors' output (see the example reported in Fig. 4, where the output of the accelerometer, gyroscope, and magnetometer of DUT1 oriented toward the Y-axis are illustrated during a thermal cycle), different approaches could be taken into account, as reported in the introduction section. Since the proposed work aims to highlight the necessity of implementing temperature compensation on real-time platform running attitude algorithms, the most complex algorithms based on artificial intelligence and digital twins have, however, been discarded. Indeed, the approaches mentioned above require the availability of experimental data in various operative conditions to obtain reliable models.

Furthermore, the expected behavior of considered sensors is linear, as can be seen in Fig. 5, and the magnetometer outputs are reported for different axes and IMUs concerning the temperature variation. Thus, even a simple compensation approach, such as adopting a linear regression model, should provide satisfactory results, and thus, it has been considered in the following analysis.

More in detail, the Curve Fitting Tool available in MATLAB has been employed. The fitting procedures may follow two different input data organizations: a fitting procedure based on each particular sensor axis and the individual DUT rather than grouping all the data relative to the respective axis collected by the different DUTs during the multiple repetitions.

Generally speaking, the first fitting procedure aims to handle the different behavior of each axis of each IMU for the temperature effects, assuring a more accurate temperature compensation but representing a complicated and expansive solution. The second solution may be viewed as a more

TABLE IV

ORIENTATION TOWARD THE *y*-AXIS. MINIMUM, MAXIMUM, MEAN, AND STANDARD DEVIATION OF (DUT2) SENSOR OUTPUTS VERSUS TEMPERATURE CYCLES

GYROSCOPE [dps]																				
	Reference				R1				R2				R3				R4			
AXIS	Min	Max	Mean	σ	Min	Max	Mean	σ	Min	Max	Mean	σ	Min	Max	Mean	σ	Min	Max	Mean	σ
x	-0.04	-0.02	-0.03	0.02	-0.14	0.12	-0.02	0.07	0.00	0.08	0.04	0.01	-0.11	0.03	-0.05	0.03	-0.10	0.10	-0.01	0.06
y	-0.11	-0.06	-0.11	0.01	-0.29	0.11	-0.08	0.09	-0.01	0.14	0.07	0.05	-0.01	0.05	0.02	0.01	-0.17	0.06	-0.08	0.08
z	-0.01	0.00	-0.01	0.03	-0.05	0.06	-0.01	0.03	-0.01	0.05	0.02	0.01	-0.01	0.05	0.02	0.01	-0.01	0.10	0.05	0.04

ACCELEROMETER [m/s^2]																				
	Reference				R1				R2				R3				R4			
AXIS	Min	Max	Mean	σ	Min	Max	Mean	σ	Min	Max	Mean	σ	Min	Max	Mean	σ	Min	Max	Mean	σ
x	0.03	0.07	0.05	0.01	-0.69	0.72	0.06	0.11	-0.85	0.69	-0.06	0.09	-0.57	0.93	0.16	0.13	-0.55	0.03	-0.26	0.05
y	5.30	10.23	9.72	0.61	4.56	10.54	9.79	0.16	5.24	10.39	9.81	0.15	5.36	10.41	9.93	0.15	-10.30	-5.21	-9.76	0.18
z	0.19	0.41	0.36	0.03	-0.99	2.07	0.39	0.18	-1.04	1.36	0.06	0.17	-0.59	1.78	0.41	0.23	-0.04	0.57	0.28	0.07

MAGNETOMETER [nT]																				
	Reference				R1				R2				R3				R4			
AXIS	Min	Max	Mean	σ	Min	Max	Mean	σ	Min	Max	Mean	σ	Min	Max	Mean	σ	Min	Max	Mean	σ
x	-28.99	-15.00	-27.54	1.72	-51.74	-14.42	-31.61	11.15	-31.72	-14.45	-27.29	2.44	-61.35	-15.37	-36.41	14.04	-46.67	-10.99	-26.52	10.25
y	-29.77	-15.29	-28.03	1.75	-40.49	-5.15	-24.47	10.40	-1.21	19.51	8.63	5.63	-32.04	10.68	-12.48	13.11	-20.95	66.70	40.30	14.99
z	8.04	15.51	14.80	0.95	1.71	21.83	13.46	4.94	43.83	97.30	83.52	7.73	-26.46	10.46	-7.28	11.29	-39.07	-12.36	-23.71	7.66

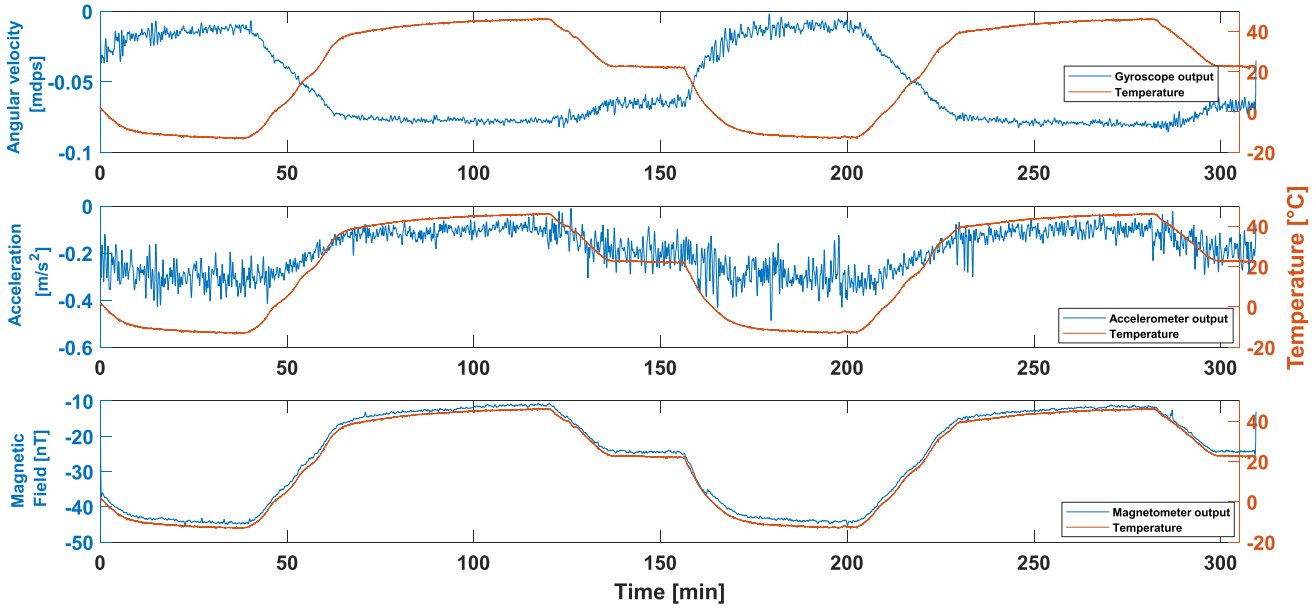

Fig. 4. Evolution of gyroscope, accelerometer, and magnetometer outputs during a single temperature cycle, in red the temperature excursion. (DUT1) The acquisition has been performed in a single direction (*X*-axis).

general approach constituting a less complicated calibration procedure, although allowing a less precise temperature compensation. The best solution should depend on the IMU platform's manufacturing quality (leading to a significant between-instruments uncertainty), the sensors' outputs, and operator needs.

In the present case study, the analysis of the magnetometer output from the three DUTs prevents the choice of temperature

TABLE V

ORIENTATION TOWARD THE Z-AXIS. MINIMUM, MAXIMUM, MEAN, AND STANDARD DEVIATION OF (DUT 3) SENSOR OUTPUTS VERSUS TEMPERATURE CYCLES

GYROSCOPE [dps]																				
	Reference				R1				R2				R3				R4			
AXIS	Min	Max	Mean	σ	Min	Max	Mean	σ	Min	Max	Mean	σ	Min	Max	Mean	σ	Min	Max	Mean	σ
x	-0.02	-0.01	-0.02	0.00	-0.09	0.09	-0.01	0.06	0.02	0.04	0.03	0.00	-0.12	0.11	-0.02	0.07	-0.10	0.02	-0.05	0.03
y	-0.10	-0.05	-0.10	0.01	-0.17	0.06	-0.08	0.08	0.01	0.12	0.08	0.04	-0.21	0.10	-0.08	0.09	-0.02	0.06	0.02	0.01
z	0.03	0.05	0.05	0.00	-0.01	0.10	0.05	0.04	0.01	0.03	0.02	0.01	-0.04	0.05	-0.01	0.03	0.01	0.04	0.02	0.01

ACCELEROMETER [m/s^2]																				
	Reference				R1				R2				R3				R4			
AXIS	Min	Max	Mean	σ	Min	Max	Mean	σ	Min	Max	Mean	σ	Min	Max	Mean	σ	Min	Max	Mean	σ
x	-0.54	-0.28	-0.51	0.03	-0.65	-0.24	-0.51	0.04	-0.31	-0.02	-0.18	0.03	-0.77	1.27	0.14	0.12	-0.67	1.17	0.16	0.16
y	0.10	0.20	0.19	0.01	-0.22	0.46	0.18	0.14	-0.38	0.11	-0.09	0.09	-0.71	0.80	0.07	0.17	-0.65	1.19	0.23	0.18
z	5.19	10.01	9.54	0.55	5.12	10.02	9.65	0.12	5.30	10.35	9.86	0.12	5.22	10.48	9.85	0.10	5.22	11.14	9.86	0.22

MAGNETOMETER [nT]																				
	Reference				R1				R2				R3				R4			
AXIS	Min	Max	Mean	σ	Min	Max	Mean	σ	Min	Max	Mean	σ	Min	Max	Mean	σ	Min	Max	Mean	σ
x	1.09	2.35	2.1	0.16	-17.04	12.01	-0.44	10.92	2.04	12.67	6.36	3.57	-18.13	16.69	1.78	9.99	-45.74	-0.76	-21.51	13.81
y	18.04	34.95	33.28	1.94	18.00	58.16	36.04	14.62	-40.02	-14.94	-34.77	4.32	-58.52	-21.06	-43.92	9.45	-58.34	-18.68	-39.81	12.23
z	-5.09	-2.37	-4.52	0.36	-17.44	3.02	-5.99	6.98	38.80	82.45	71.36	4.73	9.61	29.95	21.18	4.62	-31.52	6.52	-11.65	11.6

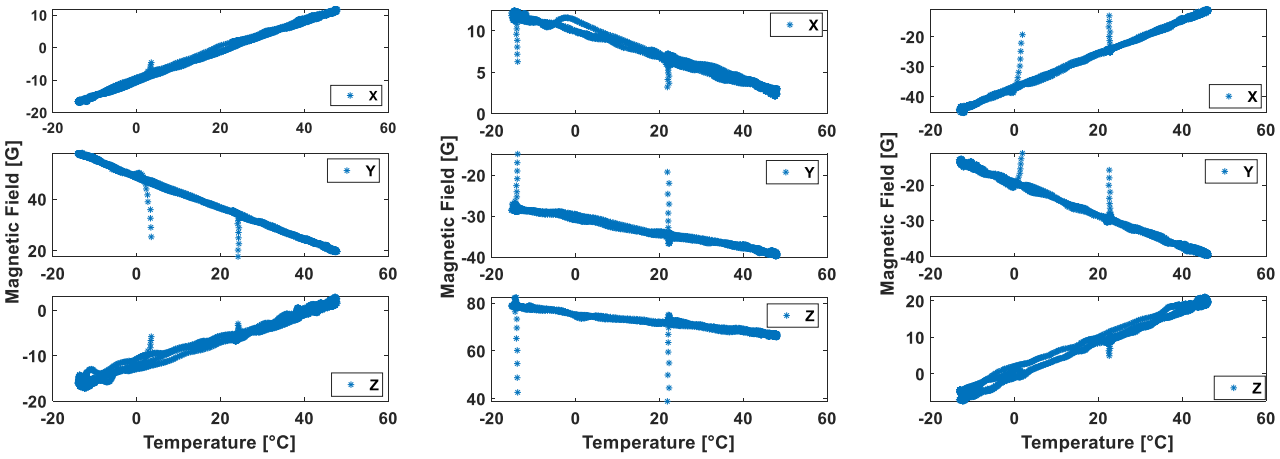

Fig. 5. Dependency of magnetometer axes on temperature variation for the three IMU considered.

compensation according to the latter approach. Indeed, the linear dependency of each sensor axis signal on the temperature is characterized by a different slope (sign) among DUTs (see x-axis behavior exhibited by the first and second IMU). In other words, the systematic effects of the temperature on the outputs of the sensors are opposite and consequently can be corrected only through an individual regression model.

Thus, the temperature compensation strategy should be based on the experimental characterization of the single IMU according to the former approach previously described (i.e., considering the data acquired during the multiple runs of test plans proposed for individual DUT and each sensor axis output).

For example, Fig. 6(a) shows the raw data acquired for the x-axis magnetometer output of DUT1 and the corresponding linear regression model, while Fig. 6(b) reports the empirical distributions (and corresponding normal fit for the compensated data). The raw data show a bi-modal distribution resulting from the temperature dependence and proposed test cycle (the tail ends of the distribution are strictly correlated

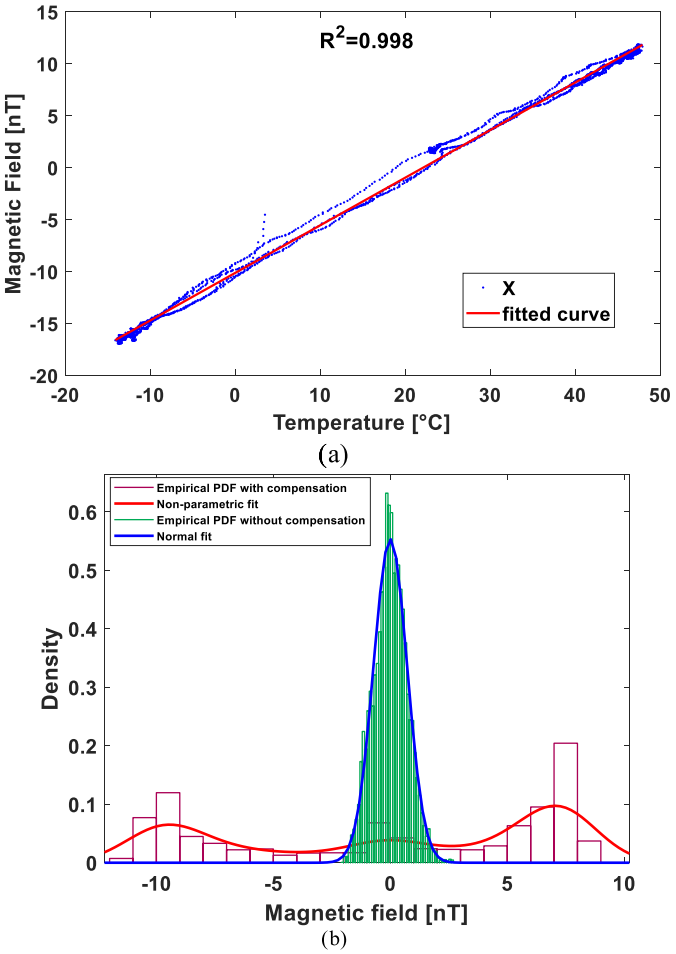

Fig. 6. Raw data for the x-axis magnetometer output of DUT1: a) linear regression model and b) empirical distributions (and corresponding normal fits) of the digital samples acquired and compensated.

with the T_H and T_C experimented), clearly due to systematic effects. On the other hand, after the compensation, the data distribution depends only on the random variability of the measurement, falling in an expected Gaussian distribution (confirmed by the X-square test). Similar considerations and results have been achieved for the other sensors, axes, and DUTs, and here not reported for the sake of readability.

VI. Estimation of Orientation

Two well-known algorithms for orientation estimation have been employed to study their behavior when fed with a low-cost IMU sensor output under a temperature stress test. The algorithms have been tested using the Navigation toolbox available in MATLAB 2021b [40]. The experiment aims to give the reader suitable guidelines for considering a possible temperature compensation and evaluate the robustness of the algorithm proposed when the temperature dependencies are not compensated. The following are the reported short descriptions of the algorithms employed.

A. Complementary Filter

The complementary filter is an orientation calculation tool presenting minimal tunable parameters, which can be optimal for systems characterized by memory constraints. In this filter, the accelerometer and the gyroscope are fused to get the orientation estimation, while the magnetometer is used for corrective purposes.

The algorithm's structure comprises a helpful low-pass filter to eliminate small forces creating disturbances in the accelerometer's reading. In contrast, a high pass filter removes the drift gathered due to the integration throughout the gyroscope data [41]. Because of simplicity, both the filter are of first order with transfer functions in La Place domain as in the following:

$$\text{LPF} = \frac{1}{1+as} \quad \text{HPF} = \frac{as}{1+as} \tag{1}$$

where a determine the cut-off frequency.

For typical MEMS sensors, the cut-off frequency is usually in the range of 2–10 Hz. For further analysis, the latter cut-off frequencies have been selected experimentally to 3 Hz to obtain the best orientation estimation.

B. AHRS Filter

The AHRS filter uses a nine-axis Kalman filter structure, employing a gyroscope, accelerometer, and magnetometer sensor output. More in detail, the algorithm aims to follow the orientation error, gyroscope offset, magnetic disturbance, and linear acceleration to calculate the orientation and angular velocity. The indirect Kalman filter models the error process with a recursive update process as described in [42] instead of tracking the orientation directly

$$x_k = \begin{bmatrix} \theta_k \\ b_k \\ a_k \\ d_k \end{bmatrix} = F_k \begin{bmatrix} \theta_{k-1} \\ b_{k-1} \\ a_{k-1} \\ d_{k-1} \end{bmatrix} + W_k \tag{2}$$

where

θ_k3-by-1 orientation error vector at time k;

b_k3-by-1 acceleration error vector measured in the sensor frame at time k;

a_k3-by-1 magnetic disturbance error vector measured in the sensor frame at time k;

d_k3-by-1 magnetic disturbance error vector measured in the sensor frame at time k;

ω_k12-by-1 additive noise vector;

F_k state transition model.

Thus, the Kalman filter assesses the system state using the current and previous states, leading to accurate orientation results; however, due to its mathematical complexity, this filter requires more computational resources with respect to the complementary filter.

C. Influence of Temperature

The runs of both the presented algorithms (when the DTU1 sensor outputs are considered) are reported in Figs. 7 and 8, showing the estimated Eulerian angles (according to the north-east-down (NED) orientation and *ZYX* frame) during the temperature excursion. For the sake of brevity, only the first two temperature cycles have been illustrated despite the

TABLE VI
MEAN VALUE AND STANDARD DEVIATION OF EULERIAN ANGLES CALCULATED ON RAW SENSORS DATA

Filter	**Complementary**						**AHRS**					
Angle	α [°]		β [°]		γ [°]		α [°]		β [°]		γ [°]	
	μ	**σ**	**μ**	**σ**	**μ**	**σ**	**μ**	**σ**	**μ**	**σ**	**μ**	**σ**
DUT #1	12,5	8,0	0,1	4,2	12,5	3,4	22,9	27,6	-1,7	14,4	22,9	18,2
DUT #2	2,0	0,6	1,3	1,2	2,0	0,5	8,1	5,2	4,4	6,7	8,1	6,2
DUT #3	11,4	4,0	2,9	2,4	11,4	5,0	-34,5	71,3	2,5	13,7	-34,5	20,3

TABLE VII
MEAN VALUE AND STANDARD DEVIATION OF EULERIAN ANGLES CALCULATED ON TEMPERATURE COMPENSATED DATA

Filter	**Complementary**						**AHRS**					
Angle	α [°]		β [°]		γ [°]		α [°]		β [°]		γ [°]	
	μ	**σ**	**μ**	**σ**	**μ**	**σ**	**μ**	**σ**	**μ**	**σ**	**μ**	**σ**
DUT #1	0,2	0,4	-0,2	0,3	0,2	0,1	-0,3	1,9	-10,3	6,7	-0,3	3,9
DUT #2	0,3	0,2	0,1	0,1	0,3	0,2	-0,1	1,1	-6,3	6,3	-0,1	4,6
DUT #3	0,0	0,2	0,4	0,5	0,0	0,4	-3,0	2,4	-2,3	2,2	-3,0	7,1

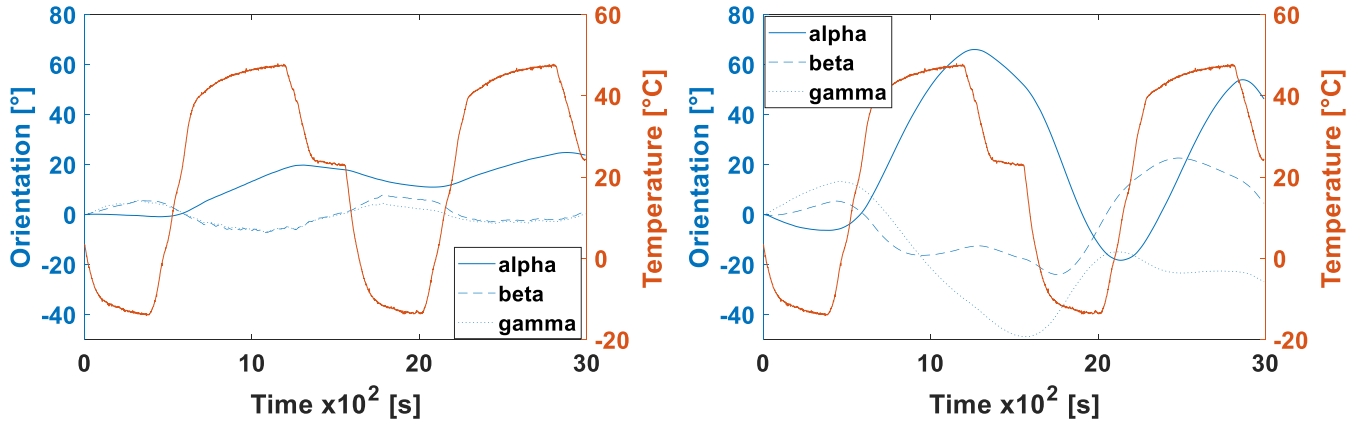

Fig. 7. Orientation estimation based on raw data through a complementary filter (left) and AHRS filter (right).

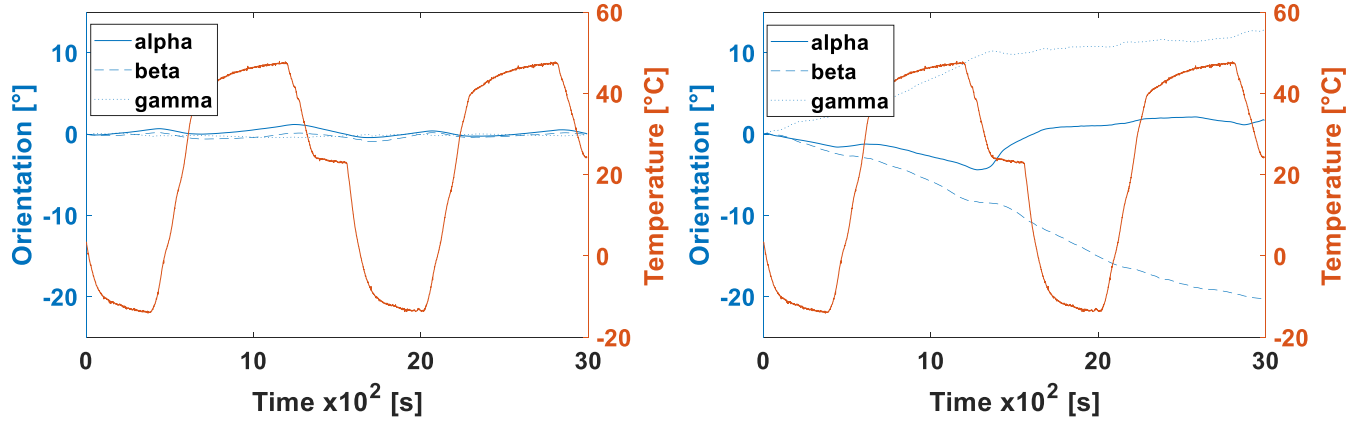

Fig. 8. Orientation estimation based on temperature-compensated data through a complementary filter (left) and AHRS filter (right).

entire profile. In Fig. 7, the results of the algorithms have been obtained considering the raw data acquired by the sensors. Quite the contrary, the temperature compensation results have been considered to estimate the device's orientation using the complementary and AHRS algorithms in Fig. 8. The numerical analysis of the Eulerian angle distributions resulting

from the test carried out for all the DUTs are summarized in Tables VI and VII. As a first observation, both the algorithms seem to be significantly influenced by the temperature changes: the variance of the estimated Eulerian angles is ever appreciable (see the corresponding columns of Table VI), with the worst behavior exhibited by the AHRS filter (probably as a consequence by the greater weight assigned to the information of the magnetometer, that is the sensor more sensitive to the temperature influence). Moreover, as can be seen from Table VII, the effects of the proposed temperature compensation are not negligible: the distributions of the estimated Eulerian angles show a smaller variation range and a smaller standard deviation with respect to the first case (when only the raw sensor data are considered). Again, the estimation through the complementary filter seems to mostly benefit from the temperature compensation with a reduction of the standard deviation greater than one order of magnitude for each Eulerian angle and each DUT.

VII. Conclusion

The authors have proposed and designed an original testbed and a test plan for the test and characterization of MEMS-based IMU with particular attention to such commercial and low-cost devices. The proposal test has been devoted to the temperature effects investigation through a repeated step test. The experimental results on real DUTs allow the temperature dependencies of the IMU sensor outputs to be highlighted in terms of systematic effects and random variability. In particular, the tests have shown the necessity of a compensation strategy considering between-instruments uncertainty and different behavior of the single axis. A linear regression model (to be calculated based on the experimental test data) is also proposed for temperature compensation of a low-cost IMU platform employed for real-time execution of mostly adopted algorithms for orientation estimation (complementary and AHRS filters). Although the adopted compensation strategy is based on a simple linear interpolation method, particularly suitable in online implementation on low-cost platforms and real-time applications), it leads to more accurate estimations of the current orientation with respect to using the raw sensor data. This aspect is highlighted by a significantly reduced standard deviation for the corresponding Eulerian angles estimated from the compensated sensor data. Further research efforts will address the influence of temperature on the dynamic application of the algorithm for the orientation estimation in navigation problems when low-cost IMU are adopted to improve the tracking of aeronautic drones.

References

[1] D. Capriglione et al., "Experimental analysis of filtering algorithms for IMU-based applications under vibrations," *IEEE Trans. Instrum. Meas.*, vol. 70, pp. 1–10, 2021.

[2] M. Straczkiewicz, P. James, and J.-P. Onnela, "A systematic review of smartphone-based human activity recognition methods for health research," *NPJ Digit. Med.*, vol. 4, no. 1, p. 148, Dec. 2021.

[3] S. Zhuo, L. Sherlock, G. Dobbie, Y. S. Koh, G. Russello, and D. Lottridge, "Real-time smartphone activity classification using inertial sensors—Recognition of scrolling, typing, and watching videos while sitting or walking," *Sensors*, vol. 20, no. 3, p. 655, Jan. 2020.

[4] S. Kaiser, Y. Wei, and V. Renaudin, "Analysis of IMU and GNSS data provided by Xiaomi 8 smartphone," in *Proc. Int. Conf. Indoor Positioning Indoor Navigat. (IPIN)*, Nov. 2021, pp. 1–8.

[5] Y. Pang et al., "Low-cost IMU error intercorrection method for verticality measurement," *IEEE Trans. Instrum. Meas.*, vol. 70, pp. 1–14, 2021.

[6] Y. Sun, X. Xu, X. Tian, L. Zhou, and Y. Li, "An adaptive zero-velocity interval detector using instep-mounted inertial measurement unit," *IEEE Trans. Instrum. Meas.*, vol. 70, pp. 1–13, 2021.

[7] D. Capriglione et al., "Performance analysis of MEMS-based inertial measurement units in terrestrial vehicles," *Measurement*, vol. 186, Oct. 2021, Art. no. 110237.

[8] D. Capriglione et al., "Experimental analysis of IMU under vibration," in *Proc. 16th IMEKO TC Conf., Testing, Diagnostics Inspection Comprehensive Value Chain Quality Safety*, Berlin, Germany, Sep. 2019, pp. 3–4.

[9] A. N. Wilson, A. Kumar, A. Jha, and L. R. Cenkeramaddi, "Embedded sensors, communication technologies, computing platforms and machine learning for UAVs: A review," *IEEE Sensors J.*, vol. 22, no. 3, pp. 1807–1826, Feb. 2021.

[10] S. Thombre et al., "Sensors and AI techniques for situational awareness in autonomous ships: A review," *IEEE Trans. Intell. Transp. Syst.*, vol. 23, no. 1, pp. 64–83, Jan. 2022.

[11] M. H. Korayem, M. Yousefzadeh, and S. Kian, "Precise end-effector pose estimation in spatial cable-driven parallel robots with elastic cables using a data fusion method," *Measurement*, vol. 130, pp. 177–190, Dec. 2018.

[12] G. Du, Y. Liang, C. Li, P. X. Liu, and D. Li, "Online robot kinematic calibration using hybrid filter with multiple sensors," *IEEE Trans. Instrum. Meas.*, vol. 69, no. 9, pp. 7092–7107, Sep. 2020.

[13] M. Ghislieri, L. Gastaldi, S. Pastorelli, S. Tadano, and V. Agostini, "Wearable inertial sensors to assess standing balance: A systematic review," *Sensors*, vol. 19, no. 19, p. 4075, Sep. 2019.

[14] M. Rana and V. Mittal, "Wearable sensors for real-time kinematics analysis in sports: A review," *IEEE Sensors J.*, vol. 21, no. 2, pp. 1187–1207, Jan. 2021.

[15] A. Schiavi, A. Prato, F. Mazzoleni, G. D'Emilia, A. Gaspari, and E. Natale, "Calibration of digital 3-axis MEMS accelerometers: A double-blind," in *Proc. IEEE Int. Workshop Metrology Industry 4.0 IoT*, Jun. 2020, pp. 542–547.

[16] Z. Wang, M. Poscente, D. Filip, M. Dimanchev, and M. P. Mintchev, "Rotary in-drilling alignment using an autonomous MEMS-based inertial measurement unit for measurement-while-drilling processes," *IEEE Instrum. Meas. Mag.*, vol. 16, no. 6, pp. 26–34, Dec. 2013.

[17] J. Otegui, A. Bahillo, I. Lopetegi, and L. E. Diez, "Evaluation of experimental GNSS and 10-DOF MEMS IMU measurements for train positioning," *IEEE Trans. Instrum. Meas.*, vol. 68, no. 1, pp. 269–279, Jan. 2019.

[18] G. Patrizi et al., "Electrical characterization under harsh environment of DC–DC converters used in diagnostic systems," *IEEE Trans. Instrum. Meas.*, vol. 71, pp. 1–11, 2022.

[19] T. Xu, X. Xu, D. Xu, Z. Zou, and H. Zhao, "Low-cost and efficient thermal calibration scheme for MEMS triaxial accelerometer," *IEEE Trans. Instrum. Meas.*, vol. 70, pp. 1–9, 2021.

[20] L. Ciani, M. Catelani, A. Bartolini, G. Guidi, and G. Patrizi, "Influence of raised ambient temperature on a sensor node using step-stress test," *IEEE Trans. Instrum. Meas.*, vol. 69, no. 12, pp. 9549–9556, Dec. 2020.

[21] T. Suppan, M. Neumayer, T. Bretterklieber, and H. Wegleiter, "Thermal drifts of capacitive flow meters: Analysis of effects and model-based compensation," *IEEE Trans. Instrum. Meas.*, vol. 70, pp. 1–11, 2021.

[22] M. Catelani et al., "Reliability and functional analysis of IMU systems under temperature-based stress tests," in *Proc. IEEE Int. Instrum. Meas. Technol. Conf. (IMTC)*, May 2021, pp. 1–6.

[23] D. Capriglione et al., "Analysis of MEMS devices under temperature stress test," in *Proc. IEEE 8th Int. Workshop Metrology Aerosp. (MetroAeroSpace)*, Jun. 2021, pp. 63–68.

[24] B. Altinoz and D. Ünsal, "Determining efficient temperature test points for IMU calibration," in *Proc. IEEE/ION Position, Location Navigat. Symp. (PLANS)*, Apr. 2018, pp. 552–556.

[25] Y. Yuksel, N. El-Sheimy, and A. Noureldin, "Error modeling and characterization of environmental effects for low cost inertial MEMS units," in *IEEE/ION Position, Location Navigat. Symp.*, May 2010, pp. 598–612.

[26] F. Hoflinger, J. Müller, R. Zhang, L. M. Reindl, and W. Burgard, "A wireless micro inertial measurement unit (IMU)," *IEEE Trans. Instrum. Meas.*, vol. 62, no. 9, pp. 2583–2595, Sep. 2013.

[27] D. Yang, J.-K. Woo, S. Lee, J. Mitchell, A. D. Challoner, and K. Najafi, "A micro oven-control system for inertial sensors," *J. Microelectromech. Syst.*, vol. 26, no. 26, pp. 507–518, Jun. 2017.
[28] G. Araghi and R. J. Landry, "Temperature compensation model of MEMS inertial sensors based on neural network," in *Proc. IEEE/ION Position, Location Navigat. Symp. (PLANS)*, Apr. 2018, pp. 301–309.
[29] Y.-H. Tu and C.-C. Peng, "An ARMA-based digital twin for MEMS gyroscope drift dynamics modeling and real-time compensation," *IEEE Sensors J.*, vol. 21, no. 3, pp. 2712–2724, Feb. 2021.
[30] R. Fontanella, D. Accardo, R. S. L. Moriello, L. Angrisani, and D. De Simone, "MEMS gyros temperature calibration through artificial neural networks," *Sens. Actuators A, Phys.*, vol. 279, pp. 553–565, Aug. 2018.
[31] B. Zhang, H. Chu, T. Sun, and L. Guo, "Thermal calibration of a triaxial MEMS gyroscope based on parameter-interpolation method," *Sens. Actuators A, Phys.*, vol. 261, pp. 103–116, Jul. 2017.
[32] J. Guo and M. Zhong, "Calibration and compensation of the scale factor errors in DTG POS," *IEEE Trans. Instrum. Meas.*, vol. 62, no. 10, pp. 2784–2794, Oct. 2013.
[33] Y. Gunhan and D. Unsal, "Polynomial degree determination for temperature dependent error compensation of inertial sensors," in *Proc. IEEE/ION Position, Location Navigat. Symp. (PLANS)*, May 2014, pp. 1209–1212.
[34] *Environmental Testing—Part 2: Tests—All Parts*, Standard IEC 60068–2, International Electrotechnical Commission, 2021.
[35] *Environmental Engineering Considerations and Laboratory Tests*, Standard MIL-STD-810G, U.S. Department of Defense, Washington, DC, USA, 2008.
[36] *JEDEC STANDARD: Temperature cycling*, Standard JESD22-A104E, JEDEC Solid State Technology, 2014.
[37] *Failure Mechanism Based Stress Test Qualification for Integrated Circuit*," document AEC-Q100-Rev-H, Automotive Electronics Council, 2014.
[38] *Environmental Engineering (EE); Environmental Conditions and Environmental Tests for Telecommunications Equipment; Part 2–5: Specification of Environmental Tests; Ground Vehicle Installations*, Standard ETSI EN 300 019–2–5, European Telecommunications Standards Institute, 2002.
[39] *Road Vehicles—Environmental Conditions and Testing for Electrical and Electronic Equipment—Part 4: Climatic Loads*, Standard ISO 16750–4, International Organization for Standardization, 2010.
[40] *Estimate Orientation Through Inertial Sensor Fusion*. Accessed: Jul. 8, 2022. [Online]. Available: https://it.mathworks.com/help/fusion/examples/estimate-orientation-through-inertial-sensor-fusion.html
[41] M. S. Islam, M. Shajid-Ul-Mahmud, T. Islam, M. S. Amin, and M. Hossam-E-Haider, "A low cost MEMS and complementary filter based attitude heading reference system (AHRS) for low speed aircraft," in *Proc. 3rd Int. Conf. Electr. Eng. Inf. Commun. Technol. (ICEEICT)*, Dhaka, Bangladesh, Sep. 2016, pp. 1–5.
[42] Y. Pititeeraphab, T. Jusing, P. Chotikunnan, N. Thongpance, W. Lekdee, and A. Teerasoradech, "The effect of average filter for complementary filter and Kalman filter based on measurement angle," in *Proc. 9th Biomed. Eng. Int. Conf. (BMEiCON)*, Laung Prabang, Laos, Dec. 2016, pp. 1–4.

Giovanni Betta (Senior Member, IEEE) was born in Napoli, Italy, in 1961. He received the M.S. degree in electrical engineering from the University of Napoli, Napoli, in 1984.

In 1989, he joined the Department of Computer Science, University of Napoli, as an Assistant Professor of electrical measurements. In 1992, he became an Associate Professor of electrical measurements with the University of Cassino, Cassino, Italy. From 2003 to 2012, he was the Dean of the Faculty of Engineering, University of Cassino. From 2015 to 2021, he was the Rector of the University of Cassino. Since 1999, he has been a Full Professor of electrical and electronic measurements with the University of Cassino, where he is currently the Vice-Rector for teaching activities. His current research interests include image-based measurement systems, sensor realization and characterization, measurement systems for fault detection and diagnosis.

Domenico Capriglione (Senior Member, IEEE) was born in Cava de' Tirreni, Italy, in 1975. He received the M.S. degree (*cum laude*) in electronic engineering from the University of Salerno, Salerno, Italy, in 2000.

He is currently an Associate Professor of electrical and electronic measurements with the University of Cassino and Southern Lazio, Cassino, Italy. His current research interests include measurements on RF and telecommunication systems, DSP-based measurement systems, instrument fault diagnosis, network measurements, and measurement of electromagnetic compatibility. In such fields, he has co-authored more than 180 scientific articles, most of which were published in relevant international journals.

Mr. Capriglione has been serving as the Chair for the IMS Technical Committee TC-37–Measurements and Networking since 2016 and an Associate Editor for *IEEE Instrumentation & Measurement Magazine* since 2022. He has been the Scientific Head of the "Time and Frequency" area for the accredited laboratory LAT105 since 2016 and the Electromagnetic Compatibility Laboratory at the University of Cassino and Southern Lazio since 2021.

Marco Carratù (Member, IEEE) received the M.S. degree in electronic engineering and the Ph.D. degree from the University of Salerno, Salerno, Italy, in 2015 and 2019, respectively.

He is currently an Assistant Professor of electronic measurements with the Department of Industrial Engineering, University of Salerno. His current research interests include instrument fault detection and isolation, sensor data fusion, digital signal processing for advanced instrumentation, artificial intelligence (AI) for instrumentation and measurement, and real-time embedded systems.

Marcantonio Catelani (Member, IEEE) received the M.S. degree in electronic engineering from the University of Florence, Florence, Italy, in 1984.

He is currently with the Department of Information Engineering, University of Florence. Strictly correlated with reliability, availability, maintainability, and safety (RAMS) are the fields of interest of both the fault diagnosis and reliability testing for components and equipment. In particular, the research activity concerns the development of test profiles used both for the characterization and the evaluation of reliability performance and, at the same time, the development of new degradation models able to estimate the life cycle of electronic components. His current research interests include development of automatic measurement systems, the characterization of A/D converters, quality control, related statistical methods, and RAMS context.

Lorenzo Ciani (Senior Member, IEEE) received the M.S. degree in electronic engineering and the Ph.D. degree in industrial and reliability engineering from the University of Florence, Florence, Italy, in 2005 and 2009, respectively.

He is currently an Associate Professor with the Department of Information Engineering, University of Florence. He has authored or co-authored more than 190 peer-reviewed journal and conference papers. His current research interests include system reliability, availability, maintainability, and safety, reliability evaluation test and analysis for electronic systems and devices, fault detection and diagnosis, and electrical and electronic instrumentation and measurement.

Dr. Ciani is a member of the IEEE IMS TC-32 Fault Tolerant Measurement Systems. He is an Associate Editor-in-Chief of the IEEE TRANSACTIONS ON INSTRUMENTATION AND MEASUREMENT and an Associate Editor of the IEEE ACCESS. He received the 2015 IEEE I&M Outstanding Young Engineer Award for "his contribution to the advancement of instrumentation and measurement in the field of reliability analysis."

Gabriele Patrizi (Member, IEEE) received the bachelor's degree (*cum laude*) in electronic and telecommunications engineering, the master's degree (*cum laude*) in electronic engineering, and the Ph.D. degree in industrial and reliability engineering from the University of Florence, Florence, Italy, in 2015, 2018, and 2022, respectively.

He is currently a Post-Doctoral Research Fellow in the field of instrumentation and measurement and an Adjunct Lecturer of electric measurements with the University of Florence. His current research interests include life cycle reliability of complex systems, condition monitoring for fault diagnosis of electronics, safety instrumented systems, data-driven prognostic, and health management.

Antonio Pietrosanto (Senior Member, IEEE) was born in 1961.

He has been a Full Professor of instrumentation and measurement with the University of Salerno, Salerno, Italy, since 2001. He has been a Founder of three spin-off companies of the University of Salerno: "SPRING OFF," "Metering Research," and "Hippocratica Imaging." His current research interests include in the fields of instrument fault detection and isolation (IFDIA), sensors, wireless sensor networks (WSNs), real-time measurements, embedded systems, metrological characterization of measurement software, advanced system for food quality inspection, and image-based measurements. He has co-authored more than 150 papers in international journals and conference proceedings.

Dr. Pietrosanto is currently the President of the Didactic Board of Electronic Engineering of UniSA.

Paolo Sommella (Member, IEEE) was born in Salerno, Italy, in 1979. He received the M.S. degree in electronic engineering and the Ph.D. degree in information engineering from the University of Salerno, Salerno, in 2004 and 2008, respectively.

In 2015, he joined the Department of Industrial Engineering (DIIn), University of Salerno, as an Assistant Professor of electrical and electronic measurements. His current research interests include instrument fault detection and isolation, measurement in software engineering, and biomedical image processing.

Open Access funding provided by 'Università degli Studi di Firenze' within the CRUI CARE Agreement